TAO, Vol. 15, No. 4, 629-645, November 2004

Analyzing the Relationship between Terminal Velocity of Raindrops and VHF Backscatter from Precipitation

Ching-Lun Su[1], Yen-Hsyang Chu[1,*] and Chun-Yi Chen[1]

(Manuscript received 14 November 2003, in final form 9 August 2004)

ABSTRACT

The exponential relationship between α and β in the expression $V_T = \alpha P^{\beta}$ was first found empirically by Chu et al. (1999), where V_T is the mean Doppler velocity of the rain drop with respect to still air, and P is the range-corrected VHF radar backscatter from precipitation. However, they did not provide a theoretical explanation for this relationship. In this article, we will show theoretically that the mathematical relationship between α and β is indeed in an exponential form, namely, $\alpha = A\exp(-\xi\beta)$, where A is the coefficient in the relation $V = AD^B$, D is the diameter of the rain drop, and ξ is a factor related to radar parameters and precipitation intensity. An examination of this exponential relationship between α and β shows that the radar experimental result was in excellent agreement with the theoretical prediction. From the observational results made with the Chung-Li VHF radar, we find that the value of β varied in the range 0.02 - 0.14, which is significantly different from the theoretical value of 0.07143. In addition, the β value is found to be positively correlated with the vertical air velocity, which is variable in nature. We, therefore, presume that the vertical air velocity seems to play a crucial factor in governing the change in the β value to explain the large scatter of the observed β values. The application of ξ value to the estimation of the precipitation intensity is also discussed in the text.

(Key words: VHF radar, Drop size distribution, Terminal velocity)

1. INTRODUCTION

It has been well recognized that a VHF radar has the advantage of accurately measuring a

[1] Institute of Space Science, National Central University, Chung-Li, Taiwan, ROC

[*] *Corresponding author address:* Prof. Yen-Hsyang Chu, Institute of Space Science, National Central University, Chung-Li, Taiwan, ROC;E-mail: yhchu@jupiter.ss.ncu.edu.tw

number of crucial precipitation-related parameters that cannot be effectively observed by radars operated at other frequencies (Larsen and Rottger 1980; Wakasugi et al. 1986; Chu et al. 1991). For example, the meteorological radar operated at frequencies of C (6 GHz) or S (3 GHz) bands cannot sufficiently detect the weak echoes from the turbulent fluctuations of atmospheric refractivity, leading to difficulty in the measurement of the vertical air velocity. Because of this, the true terminal velocity of precipitation particles cannot be obtained using meteorological radar at microwave frequency. Radars operated at frequency lower than the VHF band will have difficulty detecting precipitation echo power owing to the appreciably small ratio of the diameter of the precipitation particle to the relatively long radar wavelength, causing fairly weak precipitation echoes that are indiscernible from clear air echoes in the observed Doppler spectrum. If the radar frequency is lower than the critical frequency of the ionosphere (about 10 - 15 MHz depending on solar activity), the intense echoes reflected from the ionosphere will severely contaminate the echoes from precipitation and atmospheric refractivity fluctuations and make observations in the lower atmosphere impossible. Because echo intensities from precipitations and refractivity fluctuations at VHF band are compatible and strong enough for detection (Larsen and Rottger 1980), VHF radar is employed extensively around the world to measure atmospheric parameters in the precipitating environment.

Aside from three dimensional wind velocity and turbulence intensity, a VHF radar can measure the terminal velocity of a raindrop by carefully removing the contribution of vertical air velocity from observed Doppler velocity, provided the Doppler components of clear air echoes and precipitation echoes can be generally discerned unambiguously. This capability makes a VHF radar capable of observing the true terminal velocity of a rain drop aloft (Chu et al. 1991). In addition, from the height distribution of VHF precipitation backscatter, a bright band structure can be observed (Fukao et al. 1985; Rao et al. 1999; Reddy et al. 2002), which is an indication of the cold precipitation process responsible for the formation of raindrops below the melting layer. The drop size distribution can also be deduced from the precipitation Doppler spectrum of VHF radar by removing beam broadening and turbulent broadening effects from an observed precipitation Doppler spectrum (Wakasugi et al. 1986). With simultaneous Doppler spectra obtained by vertical and oblique radar beams, the efficiency of the drift of the hydrometeor subject to the drag of the horizontal wind can be estimated (Chu et al. 1997). A VHF radar can also be employed to investigate the inhomogeneous property of the precipitation particles distributed in the scatter volume (Chu and Song 1998). Moreover, the drift velocity of rain cells can be estimated using the spaced antenna drift method implemented in VHF radar (Reddy et al. 2002).

Except for the precipitation-related parameters and features mentioned above, the relationship between the mean terminal velocity V_T of the hydrometeor measured by the radar and the VHF radar backscatter P (or radar reflectivity factor Z) from precipitation particles have been studied by a number of researches (Chilson et al. 1993, Ulbrich and Chilson 1994, Chu et al. 1999). With VHF/UHF radars, Chilson et al. (1993) analyzed the relationship between V_T and radar reflectivity of the hydrometeors associated with a thunderstorm. Chu et al. (1999) analyzed precipitation data taken from 4 independent experiments conducted at the Chung-Li VHF radar and found that α and β values in the power-law approximation $V_T = \alpha P^{\beta}$ above the melting layer are generally smaller than those below the layer, while in

the height range of bright band the values of $\beta(\alpha)$ are enormously smaller (greater) than those above and below the bright band. In addition to the V_T-P relationships, Chu et al. (1999) found that the relationship between α and β can be empirically approximated very well to a simple exponential function $\alpha = Ae^{-\xi\beta}$, where A is the coefficient in the power-law approximation to the fallspeed -diameter relationship $V(D) = AD^B$ of precipitation particle with respect to the still air and ξ is a parameter associated with radar parameters and the properties of precipitation particles with unknown expression. Although the empirical relationship between α and β has been validated by using the Chung-Li VHF radar, no theoretical derivation of this relationship was made by Chu et al. (1999). In this article, an attempt is made to theoretically show that the relationship between α and β in the expression $V_T = \alpha P^{\beta}$ indeed is in the form of an exponential function. Moreover, the properties of α and β which are associated with atmospheric parameters, such as vertical wind velocity and the rainfall rate, are also discussed in this article.

2. THEORETICAL CONSIDERATIONS

When an electromagnetic wave is incident on a dielectric sphere with diameter D much smaller than the wavelength λ, the echoing process can be treated as Rayleigh scattering. In this case, the backscattering cross section (or echo power) of the sphere will be proportional to the ratio of D^6/λ^4 (Battan 1973). It is noteworthy that the wavelength of VHF radar is in the range 10 m to 1 m and the diameter of a rain drop is in the order of 0.08 - 0.8 cm. Therefore, the echoing mechanism of the precipitation particle for VHF radar can be regarded as Rayleight scattering. Under such conditions, the radar equation for precipitation echoes observed using a VHF radar can be formulated below (Batten 1973):

$$P_r = \frac{\varepsilon c P_t G^2 \pi^3 \tau \theta \psi |K|^2 Z}{1024 \ln 2 R^2 \lambda^2} , \tag{1}$$

where ε is the radar efficiency, P_t is transmitted peak power (W), P_r received precipitation echo power (W), c is light speed ($m\ s^{-1}$), τ is pulse width (s), λ is radar wavelength (m), G is antenna gain, θ is antenna beam width (radian) in major axis, ψ is antenna beam width (radian) in minor axis, R is the range (m), $K = (m^2 - 1)/(m^2 + 1)$, m is the complex refractive index of a rain drop, and Z is the reflectivity ($mm^6\ m^{-3}$) defined as:

$$Z = \sum D_i^6 = \int N(D) D^6 dD , \tag{2}$$

where N(D)dD is the number of precipitation particles with radius within D (mm) and D+dD per unit volume (m^3). Assume that the drop size distribution is in an exponential form (Marshall and Palmer 1948).

$$N(D) = N_0 \exp(-\delta D), \tag{3}$$

and the relation between fall speed and diameter of the rain drop is approximate to a power law (Spilhaus 1948),

$$V(D) = AD^B. \tag{3a}$$

Note that the parameter $\delta\,(\mathrm{mm}^{-1})$ in (3) represents the inverse of the mean value of D and $N_0(\mathrm{mm}^{-1}\ \mathrm{m}^{-3})$ carries the information on rain intensity, and the unit of A in (3a) is $\mathrm{m\ s}^{-1}\ \mathrm{mm}^{-B}$ and B is a dimensionless parameter. On the basis of the definition of mean terminal velocity V_T of the precipitation echoes observed by a radar $V_T = \int V(D)N(D)D^6 dD / \int N(D)D^6 dD$, from (1) we have (Chu et al. 1999)

$$V_T = \alpha P^{\beta}, \tag{4}$$

where

$$P = P_r \times R^2, \tag{5}$$

$$\beta = B/7, \tag{6}$$

$$\alpha = \frac{A\Gamma(7+B)}{\Gamma(7)(720N_0C|K|^2)^{B/7}}, \tag{7}$$

$$C = \frac{\varepsilon c P_t G^2 \pi^3 \tau \theta \psi}{1024 \ln 2 \lambda^2}, \tag{7a}$$

and $\Gamma()$ is the Gamma function. It is obvious from (4) that the unit of α is in $\mathrm{m\ s}^{-1}\ \mathrm{W}^{-\beta}\ \mathrm{m}^{-2\beta}$. Because V_T and P can be obtained from the VHF radar observations, α and β can thus be estimated by best fitting (4) to the radar-observed precipitation data. From (7), we have

$$\ln\alpha = \ln A + \ln\Gamma(7+\beta) - \ln\Gamma(7) - \beta \ln M, \tag{8}$$

where $M = 720N_0C|K|^2$. Note that the Gamma function, after taking logarithm, can be approximated to the following expression in accordance with the Stirling formula (Bender and Orszag 1978):

$$\ln \Gamma(x) = \ln(\sqrt{2\pi} x^{x-\frac{1}{2}} e^{-x}) + \frac{1}{12x} - \frac{1}{360x^2} + \ldots . \tag{9}$$

From (9), we have

$$\ln \Gamma(7+7\beta) - \ln \Gamma(7) = 6.5 \cdot [\ln(7+7\beta) - \ln(7)] + 7\beta \ln(7+7\beta) - 7\beta = -\frac{\beta}{2} + \ln(7^{7\beta}), \tag{10}$$

where the condition $\beta << 1$ has been employed in the derivation of (10) (Chu et al. 1999). Substituting (10) into (8), it reduces to

$$\ln \alpha = \ln A - 0.5\beta + 7\beta \ln 7 - \beta \ln(720 N_0 |K|^2 C). \tag{11}$$

As a result, the mathematical relation between α and β will follow an exponential function derived below:

$$\alpha = \mathrm{A}\exp(-\xi\beta), \tag{12}$$

where

$$\xi = -6.54 + \ln(N_0 |K|^2 C). \tag{13}$$

In practice, the values of A and ξ are calculated by best fitting expression (12) to the pairs of α and β in the height ranges in which the intensities of the precipitation radar returns in the respective height gate are sufficiently strong in a given duration such that the corresponding α and β values can be effectively estimated in accordance with (4). From (13), it is clear that the factor ξ is strongly related to the parameter N_0 which governs the rain drop distribution N(D) as shown in (3). Because the magnitudes of C and $|K|^2$ in (13) can be regarded as constants during the period of the radar experiment, which are the function of radar parameters and bear no relation to the precipitation, the change in N_0 will be responsible for the variation in ξ. For the Chung-Li VHF radar, because $\varepsilon = 0.15$ (assumed), $c = 3\times10^8$ m s^{-1}, $\lambda = 5.77$ m, $\tau = 2\times10^{-6}$s, $\theta = \psi = 0.129$rad, $|\mathrm{K}|^2 = 0.93$, $P_t = 120$ kW, and G = 32 dB, we have $|K|^2\mathrm{C} = 3.65\times10^9$ W m^{-1}, Consequently, from (13), it reduces to

$$\xi = 13.58 + \ln(N_0) . \tag{14}$$

Therefore, once ξ is estimated by best fitting (12) to the observed radar data, N_0 can thus be obtained in accordance with (13).

3. OBSERVATIONS AND DISCUSSION

The data employed for analysis were taken on July 9,2000, from 00 LST to 18 LST using the Chung-Li VHF radar. During this period, the center of typhoon Kai-Tak with central pressure 970 hpa was located at the southeast corner of Taiwan with a cloud system that covered the whole of Taiwan island. A rain fall rate greater than100 mm hr^{-1} was observed both by optical rain gauge and disdrometer colocated on the campus of the National Central University at a time around 15:45 LST as shown in Fig. 1, where the rain fall rate data was recorded by the optical rain gauge at sampling intervals of 30 seconds. In order to study the typhoon-related precipitation, the three independent modules of the Chung-Li VHF radar were operated simultaneously to collect the precipitation echoes and the radar parameters were set below: the nominal radar frequency was 52 MHz (corresponding to wavelength 5.77 m), interpulse period was 300 μs, pulse length was 2 μs (corresponding to range resolution of 300 m), coherent integration number was 240, delay time was 12 μs (corresponding to lowest detectable height of 1.8 km), the radar beam was steered vertically, and 40 range gates were set. The 256-point Fast Fourier Transform (FFT) algorithm was used to obtain a raw Doppler spectrum. Three raw spectra were incoherently integrated to obtain a resultant spectrum for the calculations of echo powers and Doppler velocities of the turbulent refractivity and precipitation

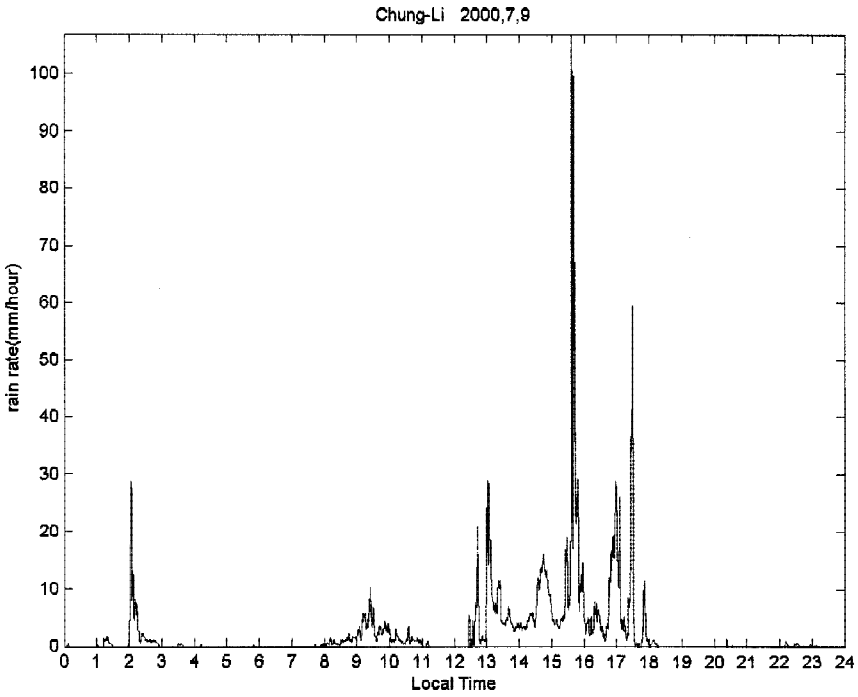

Fig. 1. Time series of rainfall rate measured by ground-based optical rain gauge at 30-second sampling intervals.

particles, provided their Doppler spectral components can be unambiguously identified and clearly separated from each other. For more detailed information on the characteristics of the Chung-Li VHF radar for precipitation measurements, refer to Chu and Lin (1994).

Figure 2 presents a typical height variation of the observed Doppler spectra for precipitation that occurred below the melting layer located at a height of about 5.5 km, in which the air density corrections (for details, see below) on the height variations of the spectral components of the precipitation echoes were made. As shown in Fig. 2, the precipitation echoes (corresponding to the spectral components with negative Doppler velocities below around 5 km) and turbulent refractivity echoes (spectral components with Doppler velocities varied around zero m s^{-1}) are clearly identified. However, it should be pointed out that, according to the results of the previous experiments carried out at the Chung-Li VHF radar (Lin 1992; Liang 1995; Chen 2000), not every precipitation Doppler spectral component can be easily distinguished from the turbulent refractivity Doppler spectral component, especially for the echoes occurred around the region of the melting layer. This is because the breadth of precipi-

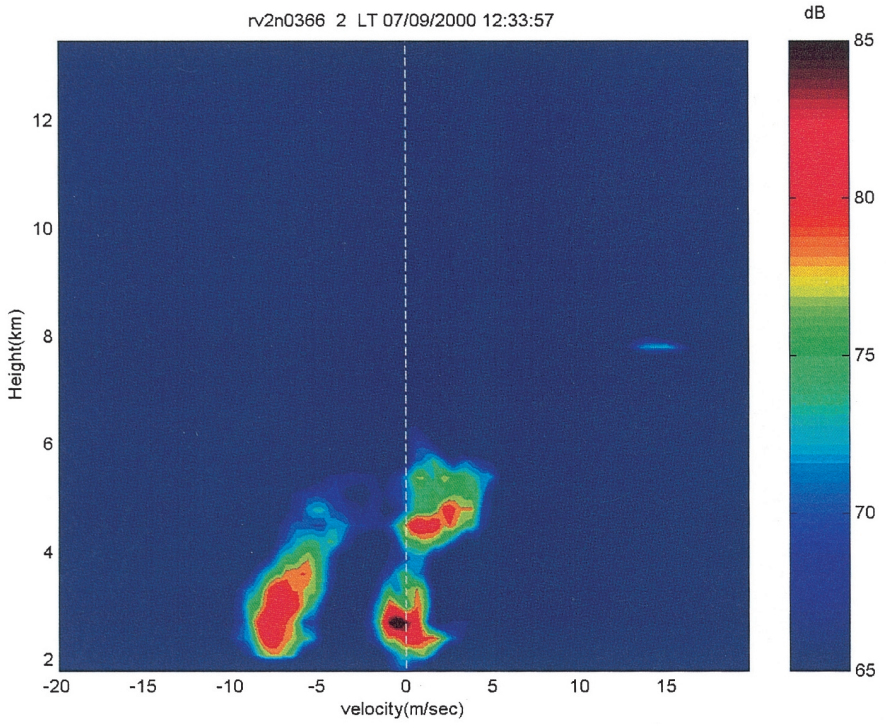

Fig. 2. Example of height variation of observed Doppler spectra for the case of the raindrops formed in the warm cloud below the melting layer, where positive (negative) velocity represents the targets moving away (toward) radar. Note that air density correction to spectral components of the precipitation echoes was made.

tation Doppler spectral component may be so wide that it covers the spectral range of turbulent refractivity due to the existence of multiple kinds of size distributions of precipitation particles in the melting layer. Other factors which may cause this difficulty in distinguishing between the precipitation and the clear air spectral components in the observed Doppler spectrum include extraordinarily intense turbulence in the scattering volume (Chen 2000), relatively weak precipitation echoes compared to turbulence refractivity echoes at VHF band, and so on. Under this situation, these data are discarded to avoid unnecessary problems. As indicated in Fig. 2, no bright band structure was observed in the profile of the precipitation backscatter, especially at a height of about 5 km which is the level of 0°C isotherm. This feature strongly implies that the raindrops were formed primarily in the region below the melting layer. Figure 2 also shows that the mean Doppler velocities of the precipitation echoes increased gradually with decreasing height, implying continuous growth of the precipitation particles during their falls in the cloud. The salient vertical air velocities were found in Fig. 2, which are believed to play a role in supplying sufficient water vapor for the formation of raindrops. Because the vertical air velocity can be directly estimated from the Doppler spectrum of turbulent refractivity, true terminal velocity of the precipitation particle can thus be obtained from the mean Doppler velocity of the precipitation echoes by removing the contribution of vertical air velocity. For the example presented in Fig. 2, the terminal velocities of the raindrops were in the range 6 - 9 m s^{-1}.

Different from the precipitation Doppler spectra presented in Fig. 2, Fig. 3 presents another type of the precipitation Doppler spectra. As shown, the height variation of the precipitation Doppler spectra can be divided into two parts, namely, the bright band structure located at around the height of 0°C isotherm (about 4.96 km at 08LT and 5.6 km at 20LT), which is characterized by intense backscatter and sudden increase in Doppler velocity with decreasing height, and the spectra located below the melting layer, which are characterized by relatively weak backscatter and a gradual decrease in Doppler velocity with decreases in height. This feature strongly indicates that the formation of the raindrops below the melting layer was directly related to the precipitation particles that originated in the region above the melting layer falling downward through the melting layer. It should be noted that one of the sufficient conditions for the formation of the bright band is small vertical air velocity (Rogers 1979). This is because strong turbulence overturning associated with strong vertical air motion would disrupt the stratification necessary for the formation of the melting layer to be well defined (Chen 2000). Moreover, intense updraft at speeds greater than about 2 m s^{-1} will suspend the dendritic ice sheets and the small overcooled droplets with diameters smaller than about 3 mm in the region above the height of 0°C isotherm (Fletcher 1962), causing the disappearance of the melting layer (Chu and Lin 1994). It is clear to see from Fig. 3 that the terminal velocity of the precipitation particles in the bright band increased with decreases in height and reaches a maximum (at about 10 m s^{-1}) at a height just below the melting layer. Below the melting layer, the terminal velocity of the raindrop decreased gradually with decreasing height. This feature clearly indicates that the precipitation particles were aggregated in the melting layer and disintegrated into smaller droplets during their falls below the melting layer, causing decreases in their terminal velocities.

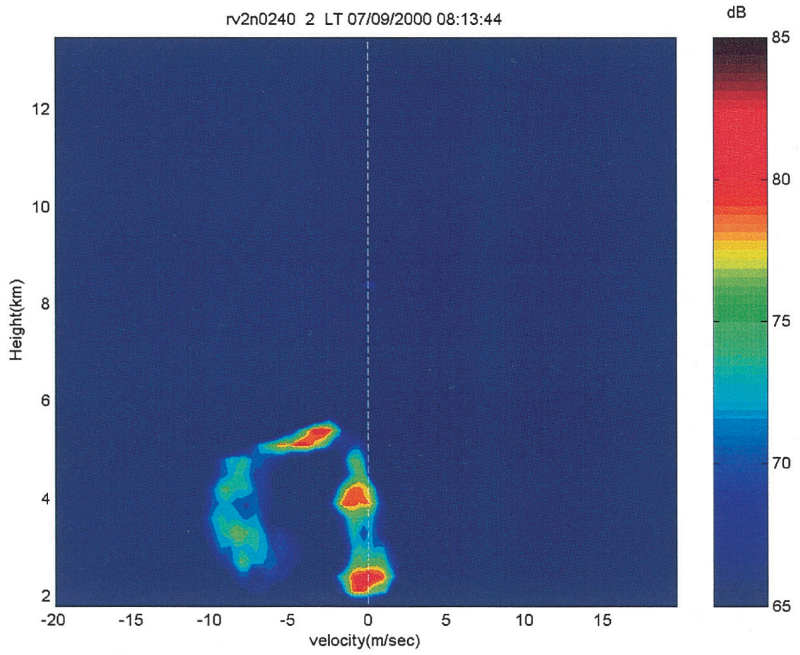

Fig. 3. Same as in Fig. 2, but for the case of the cold precipitation process. The precipitation Doppler spectral components with extraordinarily intense backscatter occurred at altitude around 5.5 km and result from melting precipitation particles in the melting layer, which corresponds to the bright band structure of the precipitation backscatter.

Once the Doppler spectral components of the precipitation and clear air are separated in the observed Doppler spectrum, their respective echo powers, mean Doppler velocities, and spectral widths can be estimated using the moment method. Figure 4 presents the height-time-intensity plot of radar backscatter from the precipitation particles that occurred in the regions above and below the freezing level. As shown, a salient bright band appeared in the height range from about 5 km to about 5.7 km, very close to the 0°C isothermal level. Inspecting Fig. 4 in more detail indicates that the central height of the bright band was higher at the time around 15 LST than that at the time around 9 LST by about 2.5 km, and after 15 LST the height gradually decreased with time. Comparing Fig.4 with Fig.1 shows that, irrespective of a time lag (approximately about 5 - 15 minutes) between the radar-measured precipitation event and the corresponding surface rainfall rate, the precipitations aloft measured by the VHF radar were in general nicely coincident with the surface rain fall rate even at intensities smaller than 0.5 mm hr^{-1} (Chu and Song 1998). Occasionally, however, one-to-one correspondence between the radar-measured precipitation and the surface rainfall rate cannot be found, such as when the surface rainfall rates occurred at 01:18 LST and around 18:00 LST, and when the

radar-measured precipitation event occurred at 03:35 LST. Presumably, the causes responsible for the non-coincidence between precipitation aloft and surface rainfall rates may be attributed to the disintegration and/or evaporation of the hydrometeor or that the height range

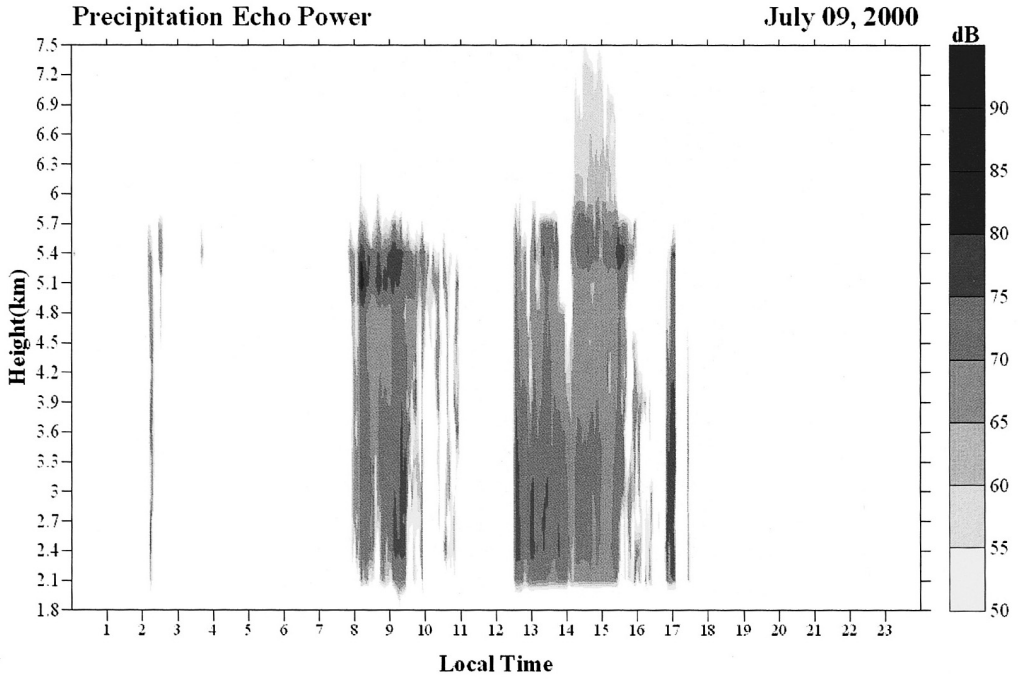

Fig. 4. Height-time-intensity plot of the radar backscatter from precipitation particles, in which the bright band structure located in the height range about 5.0 - 5.7 km is clearly seen.

where the precipitation occurs is lower than the minimum probing range of the radar. More experiments are required to clarify this question.

From the precipitation Doppler velocity and echo power, the parameters α and β in expression (4) can be estimated by least squares method. It should be noted that the power law approximation to the relationship between V(D) and D as shown in (3a) is applicable near the ground surface. If this expression is employed at other altitudes, a correction factor should be multiplied to the right hand side of (3a) so that the effect of atmospheric drag on the terminal velocity can be corrected. Although a number of correction factors have been proposed by a number of investigators, the factor $(\rho_0/\rho)^{0.4}$ is used in this article (Foote and du Toit 1969; Atlas et al. 1973), where ρ_0 and ρ are, respectively, the air densities at the ground and at the level of radar observation. Figs. 5a and b present the scatter diagrams of range-corrected pre-

cipitation echo power versus density-corrected terminal velocity for the radar data taken on July 9, 2000, 07:40 LST - 08:10 LST in the height range 2.1 - 3.6 km and 3.9 - 5.4 km, respectively. Note that the radar-observed precipitation data at 1.8 km with abnormally weak echo powers were discarded because they suffer from radar system effects. As shown in Figs. 5a, b, positive correlations between precipitation backscatter and terminal velocity in the height range 2.1 - 4.8 km were observed, and the correlations at height 5.1 and 5.4 km were negative. Note that, on the basis of Pan-Chiao radiosonde data, the levels of 0°C isotherm at 08 LST and 20 LST were, respectively, at about 4.99 and 5.57 km. Namely, it is very likely that the precipitation particles in the height range 5.1 - 5.4 km consisted of different types of hydrometeors, including melting ice particles, super-cooled liquid droplets and solid ice crystal particles. If it is the case, the assumption of single drop size distribution as described in (3) will be invalid, and, as a result, the power law relationship between terminal velocity and precipitation backscatter as shown in (4) will not be applicable (Chu et al. 1999). In order to

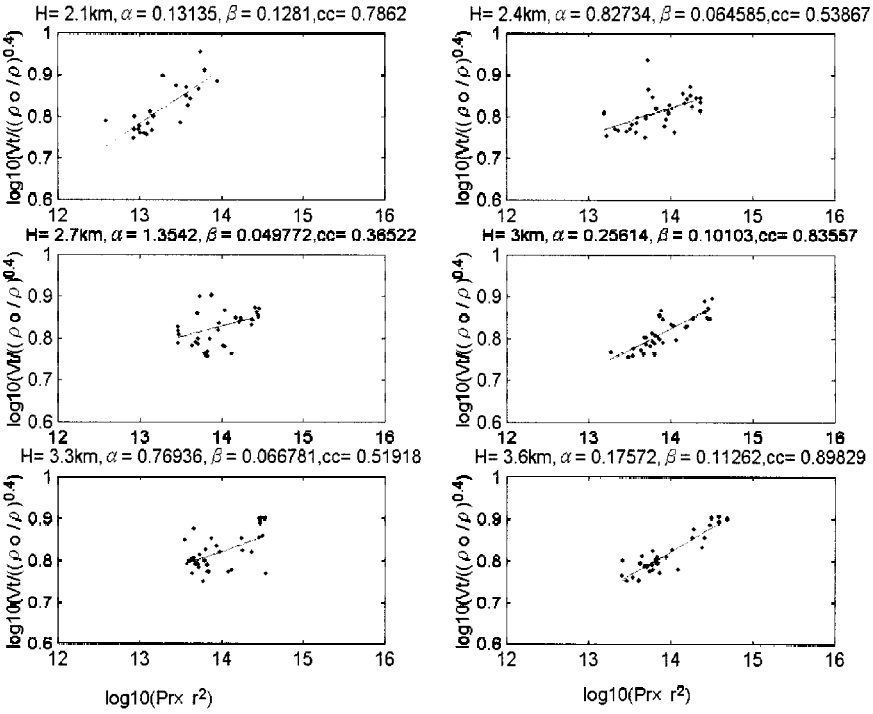

Fig. 5a. Scatter diagram of range-corrected precipitation echo power versus density-corrected terminal velocity for the radar data taken on July 9, 2000, 07:40 LST - 08:10 LST in the height range 2.1 - 3.6 km. The parameter cc located at the upper corner of each panel represents the correlation coefficient between precipitation echo power and terminal velocity.

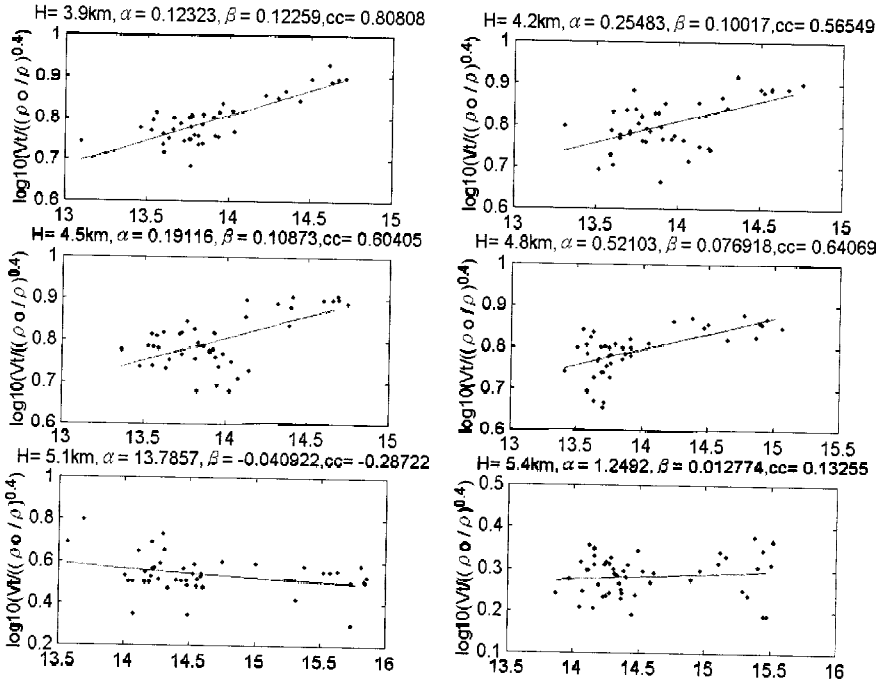

Fig. 5b. Same as in Fig. 3a, but for data in the height range 3.9 - 5.4 km.

avoid this problem, the data above the melting layer will not be adopted for the analysis of the α - β relationship.

Figure 6 compares the observed (marked with open circles) and theoretical relationship between α and β, in which the data are taken from Figs. 4a and 5b and the solid curve is the best fit to the data in accordance with (12). It is clear from Fig. 6 that the observed α - β relationship is in an excellent agreement with the theoretical prediction, validating the applicability of (12).

When a spherical raindrop falls in still atmosphere at terminal velocity, the balance between gravity and air drag forces governing its fall will be reached. Under this condition, the terminal velocity can be theoretically estimated in accordance with following expression (Gunn and Kinzer 1949; Rogers 1979):

$$V_T = \sqrt{\frac{4g(\rho_s - \rho)}{3\rho\mu}} D^{0.5}, \tag{15}$$

where ρ and ρ_s are, respectively, the air and raindrop densities, μ is atmospheric drag coefficient, g is gravity acceleration, and D is the diameter of the raindrop. A comparison of

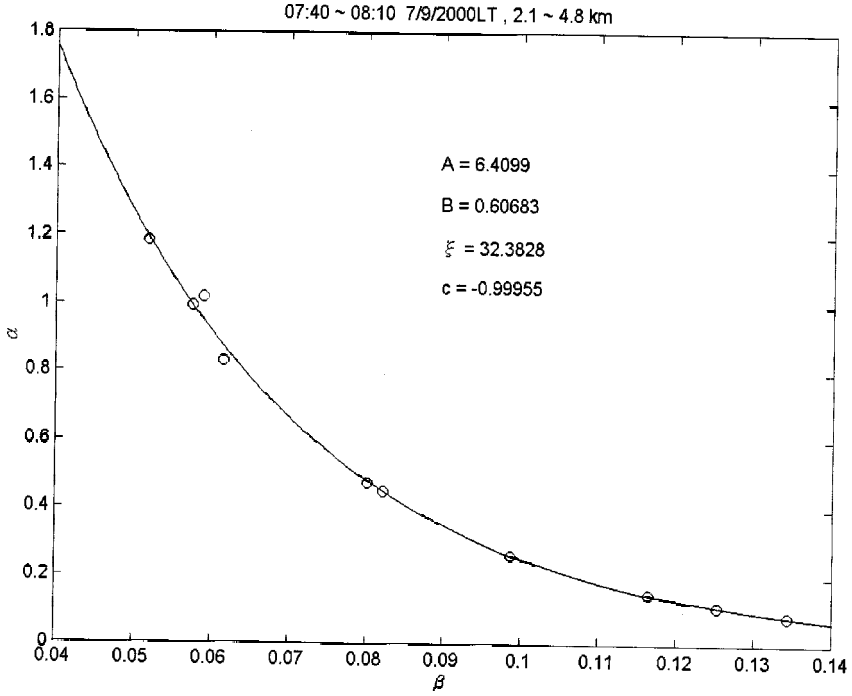

Fig. 6. Comparison of observed (marked with open circles) with theoretical relationship between α and β, in which the observed data are taken from Figs. 3a and b and the solid curve is the best fit to the data in accordance with (12).

(15) with (3a) reveals that the theoretical value of power B in (3a) will be 0.5, leading to the magnitude of β in (4) and (6) is equal to 0.07143 and the theoretical value of A in (3a) will be $\sqrt{4g(\rho_s - \rho)/3\rho\mu}$. However, the results of the practical radar experiments shown in Figs. 3a , b and reported elsewhere (e.g., Liu and Orville 1968; Sekhon and Strivastava 1971; Chu et al. 1999) indicate that the observed values of β for the raindrops are appreciably diverse in the range 0.02 - 0.14 and seldom equal to the theoretical value of 0.07143. It should be noted that a number of assumptions implicitly made in the derivation of (12) with a β value of 0.07143 include a single drop-type distribution which does not change during the fall of the raindrop, a non-turbulent environment, a fixed shape of the raindrop, and no deformation effects on the raindrop due to pressure differences between the lateral, upper and bottom sides of the drop. It is expected that changes in the assumptions that are made in the derivation of (4) will result in a change in β value that may be significantly different from the theoretical value of 0.07143. It would be important and interesting to study a plausible relationship between vertical air velocity and the β value. Figure 7 presents a scatter diagram of β values versus vertical air velocity, in which the radar data were carefully selected for the comparison. As shown, a

positive correlation between β values and vertical velocity is seen. From the regressive line of best fit to the data, the magnitude of B in (3a) for the condition of zero vertical velocity is 0.49 (corresponding to β value of 0.06974), which is very close to the theoretical value of 0.5 as shown in (15). Therefore, Fig. 7 provides concrete evidence that vertical air velocity plays a crucial role in the determination of the value of β estimated from the radar-observed Doppler velocity of the precipitation particles and precipitation backscatter. This result suggests that great caution should be taken in the interpretation of the behavior of β values in precipitation environments with variable vertical air velocity.

From (13), it is clear that the value of ξ in (12) is proportional to $\ln(N_0)$, and, as a result, it seems that the magnitude of N_0 can be directly estimated from ξ. However, except for N_0, ξ is also a function of C and $|K|^2$. Although K is a constant for liquid raindrops, the magnitude of C is governed by the radar parameters which include the radar transmitted peak power, antenna gain, antenna beam width, radar wavelength, radar pulse length, and the radar efficiency ε as shown in (7a). Note that the correct values of these parameters can be obtained only after the characteristics of the whole radar system are carefully calibrated. Therefore, the estimation of N_0 in terms of ξ is irrelevant before the radar system is calibrated to obtain

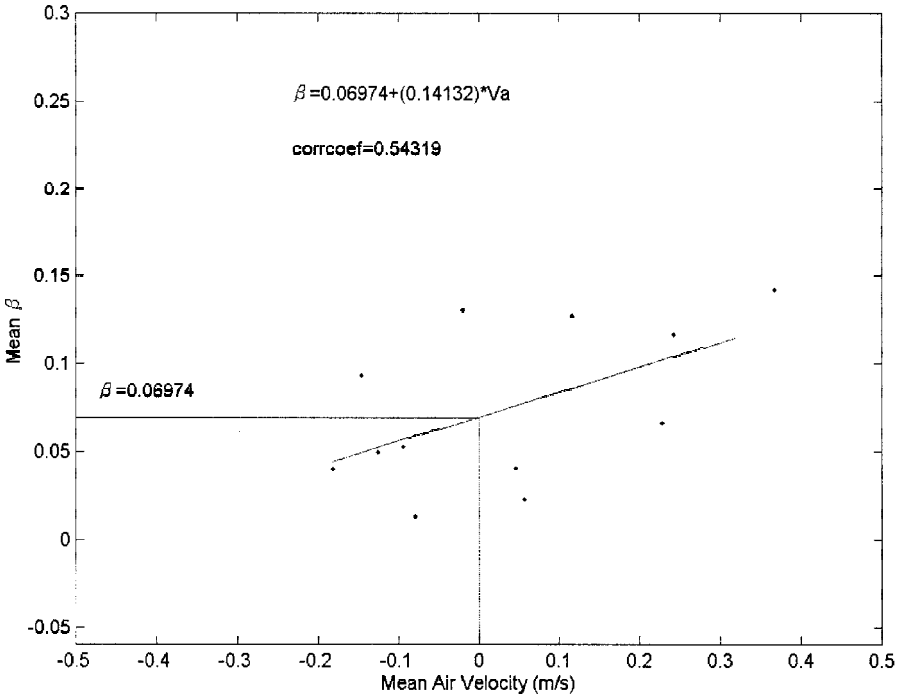

Fig. 7. Scatter diagram of β value versus vertical air velocity. Note that the β value of 0.06974 corresponds to the B value of 0.49 in accordance with (6).

accurate radar parameters. Nevertheless, it is expected that the ξ value will be directly related to the rainfall rate R due to the close connection between R and N_0. The definition of the rainfall rate R is given by

$$R = \frac{\pi}{6} \int N(D) D^3 V(D) dD. \tag{16}$$

Substituting (3) and (3a) into (16), we have

$$R = \frac{\pi A N_0 \Gamma(B+4)}{6\delta^{B+4}}. \tag{17}$$

Therefore, N_0 will be linearly proportional to R if the parameters A, B, and δ are all constant. Figure 8 shows the scatter diagram of estimated ξ value versus mean rainfall rate measured by the ground-based optical rain gauge, where each data point represents a 30-minute average and cc represents the correlation coefficient. It is clear from Fig. 8 that, irrespective of a relative low correlation (only 0.38) between ξ and R, the main body of the data point shows a

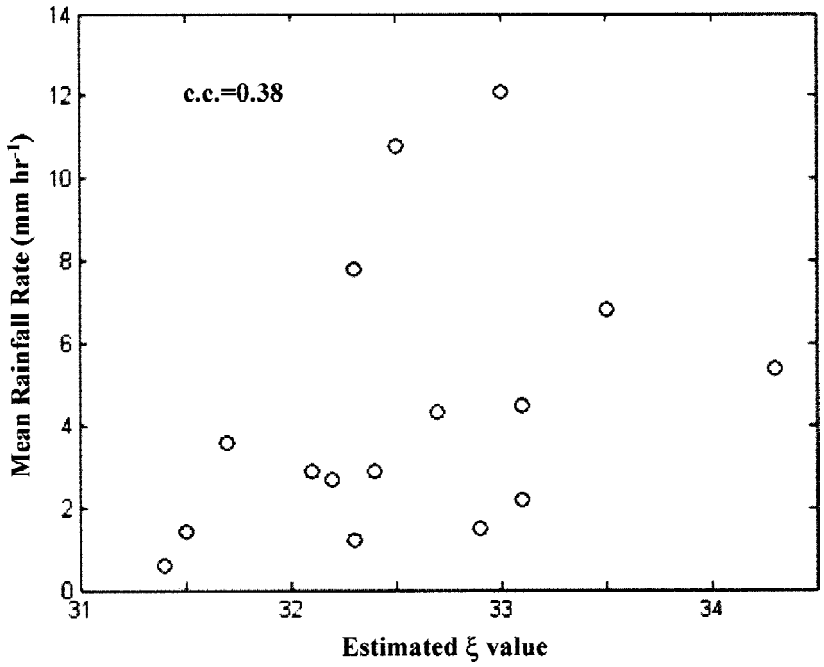

Fig. 8. Scatter diagram of estimated ξ value in accordance with (12) through the least squares fit versus mean rainfall rate measured by ground-based optical rain gauge, where each point shown in the figure was calculated on the basis of the respective data in a period of 30 minutes and cc represents the correlation coefficient.

trend of positive correlation between the two, in general agreement with the theoretical expectations as shown in (14) and (17).

4. CONCLUSION

In this article, an analytical expression describing the relationship between the parameters α and β in the power law relation $V_T = \alpha P^{\beta}$ is derived and we show that the α-β relationship is indeed in the form of an exponential function, validating the empirical relationship first reported by Chu et al. (1999). With the theoretical α-β relationship, the coefficient N_0 in the exponential drop size distribution $N_0 \exp(-\delta D)$ can be estimated by best fitting expression (12) to the radar data. Experimental results obtained by the Chung-Li VHF radar show that the radar-measured α-β relationships were in excellent agreement with the theoretical predictions, and, as expected, the estimated ξ value in the power-law relation $\alpha = A \exp(-\xi\beta)$ is proportional to the observed rain fall rate. We also find that the β value is positively correlated with vertical air velocity. This feature strongly implies that the atmospheric dynamic behavior may play a crucial role in determining the fall speed-size diameter relationship of the raindrop.

Acknowledgements This work was supported by National Science Council, R.O.C., under grant NSC92-2111-M-008-001.

REFERENCES

Atlas, D, R. C. Srivastava, and R. S. Sekhon, 1973: Doppler radar characteristics of precipitation at vertical incidence. *Rev. Geophys. Space Phys.*, **11**, 1-35.

Battan, L. J., 1973: Radar observations of the atmosphere. Univ. of Chicago Press, Chicago, III, 324 p.

Bender, C. M., and S. Orszag, 1978: Advanced mathematical methods for scientists and engineers. McGraw-Hill, Inc., New York.

Chen, M. Y., 2000: Study of the relation between terminal velocity and drop size distribution of the hydrometeor associated with convective system using the Chung-Li VHF radar. Master thesis, National Central Univ., Taiwan, R.O.C. (in Chinese)

Chilson, P. B., C. W. Ulbrich, M. F. Larsen, P. Perillat, and J. E. Keener, 1993: Observations of a tropical thunderstorm using a vertically pointing, dual-frequency, collinear beam Doppler radar. *J. Atmos. Oceanic Technol.*, **10**, 663-673

Chu, Y. H., T. S. Hsu, L. H. Chen, J. K. Chao, C. H. Liu, and J. Rottger, 1990: A study of the characteristics of VHF radar echo power in the Taiwan area. *Radio Sci.*, **25**, 527-538.

Chu, Y. H., and L. P. Chian, 1991: Investigation of atmospheric precipitations by using Chung-Li VHF Radar. *Radio Sci.*, **26**, 717-729.

Chu, Y. H., and C. H. Lin, 1994: Severe depletion of turbulent echo power in association with precipitation observed by using Chung-Li VHF Radar. *Radio Sci.*, **29**, 1311-1320.

Chu, Y. H., T. Y. Chen, and T. H. Lin, 1997: An examination of the wind-driven on the drift of precipitation particles using the Chung-Li VHF Radar. *Radio Sci*., **32**, 957-966.

Chu,Y. H., and J. S. Song, 1998: Observation of precipitation associated with cold front using VHF wind profiler and ground-based optical raingauge. *J. Geophys. Res*., **103**, 11401-11409.

Chu, Y. H., S. P. Shih, C. L. Su, K. L. Lee, T. H. Lin, and W. C. Liang, 1999: A study on the relation between terminal velocity and VHF backscatter from precipitation particles using the Chung-Li VHF Radar. *J. Appl. Meteor*., **38**, 1720-1728.

Foote, G., and P. S. du Toit, 1969: Terminal velocitiy of raindrops aloft. *J. Appl. Meteor*., **8**, 585-591.

Fukao, S., K. Wakasugi, T. Sato, T. Tsuda, I. Kimura, N. Takeuchi, M. Matsuno, and S. Kato, 1985: Simultaneous observation of precipitating atmosphere by VHF and C/Ku band radars. *Radio Sci*., **20**, 622-630.

Gunn, R., and G. D. Kinzer, 1949: The terminal velocity of fall for water droplets in stagent air. *J. Meteor*., **6**, 243-248.

Larsen, M. F., and J. Rottger, 1987: Observation of thunderstorm reflectivities and doppler velocities measured at VHF and UHF. *J. Atmos. Oceanic Technol*., **4**, 151-159.

Liang, W. C., 1995: Observations of frontal precipitation using the Chung-Li VHF radar. Master thesis, National Central Univ., Taiwan, R.O.C. (in Chinese)

Lin, C. S., 1992: On the study of the charactersiitcs of the precipitating atmosphere using the Chung-Li VHF radar. Master thesis, National Central Univ., Taiwan, R.O.C. (in Chinese)

Liu, J. Y., and H. D. Orville, 1968: Numerical modeling of precipitation effects on cumulus cloud. Rept. 68-9, Inst. Atmos. Sci., South Dakoda School of Mines and Technology, Rapid City, 70p.

Marshall, J. S., and W. M. Palmer, 1948: The distribution of raindrops with size. *J. Meteor*., **5**, 165-166.

Rao, T. N., D. N. Rao, and S. Raghavan, 1999: Tropical precipitating systems observed with Indian MST radar. *Radio Sci*., **34**, 1125-1139.

Reddy, K., S. P. Shih, and Y. H. Chu, 2002: A study of precipitating cloud system using Chung-Li VHF radar. *Radio Sci*., **37**, No. 4, 1067, dio: 10.1029/2000RS002544.

Rogers, R. R., 1979: A short course in cloud physics, Pergamon Press, New York, 2nd edition, 235p.

Sekhon, R. S., and R. C. Strivastava, 1971: Doppler radar observations of drop-size distributions in a thunderstorm. *J. Atmos. Sci*., **28**, 983-994.

Spilhaus, A. F., 1948: Raindrop size, shape, and falling speed. *J. Meteor*., **5**, 108-110.

Ulbrich, C. W., and P. B. Chilson, 1994: Effects of variations in precipitation size distribution and fallspeed law parameters on relations between mean Doppler fallspeed and reflectivity factor. *J. Atmos. Oceanic Technol*., **11**, 1656-1663.

Wakasugi, K., A. Mizutani, M. Masaru, S. Fukao, and S. Kato, 1986: A direct method for deriving drop-size distribution and vertical air velocities from VHF doppler radar spectra. *J. Atmos. Oceanic Technol*., **3**, 623-629.